JOURNAL OF CATALYSIS **178,** 533–539 (1998)
ARTICLE NO. CA982188

A Comparative Study of *n*-Pentane and *n*-Butane Isomerization over Zirconia-Supported Tungsten Oxide: Pulse and Flow Studies and DRIFTS Catalyst Characterization

Lucía M. Petkovic, James R. Bielenberg, and Gustavo Larsen[1]

Department of Chemical Engineering, University of Nebraska, Lincoln, Nebraska 68588-0126

Received December 18, 1997; revised June 8, 1998; accepted June 22, 1998

The reactions of *n*-pentane and *n*-butane over both tungstated zirconia (WZ) and platinum supported on tungstated zirconia (PtWZ) in the presence of hydrogen were studied in the pulse mode. Influence of contact time at 666 kPa, and *n*-pentane flow mode results in an atmospheric pressure packed-bed reactor are reported. The diffuse reflectance infrared (DRIFTS) spectra of adsorbed CO on PtWZ and the tungsten oxide-free sample are compared. The WZ sample was found to be unable to retain CO at room temperature. The behavior of W-O vibrations before and after reduction is also discussed. Acid cracking and isomerization pathways appear to occur on different active sites, in light of pulse experiments. The presence of Pt produces an increase in the number of isomerization sites, but has no obvious positive influence on catalyst deactivation. In addition, it does not promote cracking, but metal-catalyzed hydrogenolysis (internal C-C bond rupture) instead. The isomerization of *n*-pentane may follow a unimolecular pathway, as seen by the absence of C_6 disproportionation species in the flow mode experiments.

Key Words: **tungstated zirconia; alkane isomerization; CO DRIFTS.**

INTRODUCTION

Strong solid acids as catalysts for hydrocarbon isomerization reactions are currently sought because they have the potential to offer key advantages over liquid acids such as less corrosion, much easier handling and storage, and the design simplicity of packed beds. The development of strong solid acid catalysts for low molecular weight alkane isomerization reactions is an active field of research (1). Despite their relatively high activity, sulfated zirconia (SZ) based catalysts undergo partial loss of the sulfate function during catalyst calcination, regeneration or reduction, deactivation by coke formation, and poisoning of the metal function due to sulfate reduction under reducing atmospheres (2). Zeolites have also been used for such hydrocarbon conversion reactions, but it is still difficult to achieve good isomerization yields at relatively low temperatures, especially for small normal paraffins (3). Zirconia-supported Mo- and W-based oxoanions (MoZ and WZ) were originally proposed by Hino and Arata (4,5). They appear to be suitable candidates for isomerization of alkanes heavier than C_4. In particular, the tungstated zirconia system has also been proposed as a good acidic carrier to support noble metals such as platinum in order to obtain active reforming catalysts (6).

Tungstated zirconia has less tendency to decompose during oxidation–reduction cycles than SZ, and platinum supported on tungstated zirconia (PtWZ) shows a much higher isomerization selectivity for heavier alkanes such as *n*-heptane than platinum supported on sulfated zirconia (PtSZ) (7). Low tendency to form coke (8) and good isomerization activity, as well as selectivity, make PtWZ catalysts a promising system in the 470–570 K range.

In this paper, we compare the behavior of PtWZ and WZ for *n*-pentane and *n*-butane isomerization at 666 kPa in the pulse mode, to assess the differences in reactivity and selectivity between these two hydrocarbons under the same experimental conditions. From a fundamental viewpoint, studies dealing with the catalytic behavior of clean PtWZ and WZ surfaces are still lacking. One of the main goals for this contribution was to demonstrate that isomerization, acid cracking, and metal-catalyzed hydrogenolysis should in principle take place over different active sites, which in turn are executed to deactivate in different ways. The most active sites, which are likely to account for a substantial fraction of the carbon deposited at short times on stream, can only be probed by pulse techniques. While we are aware of the difficulties associated with trying to link steady state behavior with pulse reactor performance, the former provides valuable practical information, but little or no knowledge of the active surface species present, prior to carbon deposition.

We also included atmospheric pressure, continuous flow results on *n*-pentane isomerization over these two catalysts and compare these results with our previous work on

[1] To whom all correspondence should be addressed. E-mail: glarsen@unlinfo.unl.edu.

0021-9517/98 $25.00

n-butane isomerization in the flow mode. We have chosen *n*-pentane, not only because of the anticipated simplicity in its product distribution, but also because it represents, unlike *n*-butane, the first *n*-paraffin capable of undergoing unimolecular skeletal rearrangements (9). In previous studies, we observed evidence for disproportionation products (C_3 and C_5) in the isomerization of *n*-butane over PtWZ (10). From a fundamental viewpoint, it appears interesting to measure the activation energies for the different products observed in both reactions and to check whether the disproportionation pathway is also a possibility in the *n*-pentane/H_2 reaction network. We note that this has been observed in the much more active (and less stable) iron-manganese sulfated zirconia system (11). In addition, two previous observations were further explored by means of diffuse reflectance infrared (DRIFTS) methods. First, we have previously reported on the low CO chemisorption capacity of PtWZ catalysts (8). This could in principle be due to either low dispersions or partial coverage of the Pt surface by WO_x patches. Second, the intense blue coloration of spent catalysts reminded us of the typical behavior of electrochromic tungsten oxide centers (12). A study of the infrared bands in the 1100–800 cm^{-1} range should in principle shed some light on this issue.

Even though it is now known that isomerization species will dominate the product distribution at long times on stream (13), the selectivity may be dramatically different on the clean surface. Our working hypothesis was that cracking products could influence catalyst deactivation during the initial reaction stages. Pulse techniques have been used in the past to measure the reactivity of clean surfaces (14–16).

EXPERIMENTAL

The catalyst preparation method is described elsewhere (8). In brief, hydrous zirconia obtained by precipitation of $ZrOCl_2 \cdot 8H_2O$ (Aldrich) with concentrated ammonia was impregnated with a solution of $(NH_4)_6W_{12}O_{39} \cdot xH_2O$ (Aldrich) to form the precursor for tungstated zirconia catalysts (WZ). This catalyst precursor was subsequently impregnated with an aqueous solution of $PtCl_6H_2 \cdot xH_2O$ (Aldrich) to form the platinum tungstated zirconia catalysts (PtWZ) starting material. Subscripts indicate the nominal amount in wt% of each component. For example, $Pt_{0.3}W_{12}Z$ refers to a catalyst containing 0.3 wt% platinum and 12 wt% WO_3.

A stainless steel dual pulse/flow reaction system equipped with Brooks 5880 mass-flow controllers and a quartz U-tube packed bed reactor was used for the present studies. The reactor, which contained an inert α-alumina or quartz preheating bed, was loaded with 0.700 g of catalyst in the form of 20–45 mesh particles for both pulse and flow experiments. The bed-packing density was found to be 1.9 g/cc, resulting in a reactor volume of 0.37 cc. Visual inspection revealed that the 20–45 mesh particles were very irregular in both size and shape. Therefore, we opted to report contact times based on total reactor volume, rather than on a void fraction that is rather difficult to measure or estimate accurately. We attempted to measure the apparent solid density by massing a large number of catalyst pellets, but the variance of such measurements did not warrant a precise determination of the void fraction. All catalyst precursors were calcined *in situ* in air at 1096 K for 1 h, followed by reduction at 623 K under flowing hydrogen for another hour. Ultra high purity gases (UHP, Linweld®) and *n*-pentane HPLC grade (Aldrich®) were used in all experiments. The *n*-pentane stream was produced by passing mass-flow controlled UHP helium through a bubbler kept at 273 K by means of complete immersion in an ice-water bath. The reaction temperature was controlled to ±0.5 K. The hydrocarbon pulses were injected upstream the reactor by means of a manual 6-way GC valve from Valco®. We calculated the hydrocarbon injection amounts, based on the volumes of the two injection loops used in each case and on the loop loading pressure (atmospheric). The amount of *n*-butane injected was 0.67 micromoles, and that of *n*-pentane was 0.52 micromoles. The importance of these two numbers lies in the fact that they are much smaller than the total amount of tungsten in the catalyst bed (360 μmoles, by about four orders of magnitude), even if we assume that only a small fraction of the latter may be responsible for the catalysis. Therefore, it was a priori possible to probe the most active sites, while keeping coke production to very low levels. Product analysis was conducted on-line using GC (HP 5880A, methyl silicone capillary column, FID) detection.

In order to evaluate whether our data represents kinetics, rather than mass and heat transfer effects, our reaction results were analyzed in terms of the Weisz-Prater (17), and the Mears (19) criteria. Diffusivity, porosity, and tortuosity data were calculated, or estimated as worst scenarios (18). The bulk concentrations of butane and pentane were assumed as those resulting from pressurization of the pulse to 666 kPa, without dilution. Enthalpies of reaction were estimated from heat of formation data. Both criteria were satisfied by all runs, leading us to assume negligible intraparticle mass transfer effects (Weisz-Prater) and negligible interphase heat and mass transfer (Mears).

Experiments to gather data for activation energy calculations were collected in a sequence of decreasing temperatures and at low conversions. Two points were collected at each temperature, resulting in a total of 6 to 10 points per fit. For the *n*-butane reaction, the experiments were done in the range 533–563 K while keeping total conversion below 2.7 wt% and 7.7 wt%, for the $W_{12}Z$ and the $Pt_{0.3}W_{12}Z$ catalysts, respectively. For the *n*-pentane reaction, the temperature range was 523–541 K and 488–528 K, for the $W_{12}Z$

and the $Pt_{0.3}W_{12}Z$ catalysts, respectively. Conversion was kept below 1.8 wt% for the reaction of *n*-pentane on $W_{12}Z$, but because the $Pt_{0.3}W_{12}Z$ catalyst showed to be more active and selective to isopentane production than its Pt-free counterpart, the total conversion was allowed to reach up to 18% in isopentane (i.e., at the highest temperature considered) to afford detection of lower alkanes. This was the only case were the 10% total conversion rule-of-thumb for differential reactors was broken, and, therefore, the activation energy value for isopentane production over the Pt-containing catalyst may be somewhat in error.

Carbon monoxide chemisorption and BET surface area measurements were carried out in a conventional Pyrex® volumetric system using standard static methods. The custom-built adsorption apparatus is equipped with a Baratron® pressure transducer, greaseless stopcocks, and mechanical and diffusion pumps. All samples used in this study gave specific surface areas in the range 28 ± 1 m^2/g.

The DRIFTS studies were performed on a Nicolet® 20 SXB Fourier transform infrared spectrometer equipped with a commercial DRIFTS catalyst chamber and optical and temperature control system from Spectratech®. The catalyst samples used in DRIFTS studies had been previously calcined at 1096 K in flowing air, following the same protocol as that for the samples used in the reaction experiments. *In situ* reactivation at 873 K and reduction at 573 K was carried out in the DRIFTS catalyst chamber. Carbon monoxide was allowed in the DRIFTS reaction cell until saturation, followed by a purging period with UHP nitrogen to remove weakly adsorbed species. For comparison purposes, a platinum-zirconia (PtZ) sample was prepared following the same procedure as that for the catalysts. A background subtraction (400 scan, resolution 4 cm^{-1}) for each spectrum was conducted by collecting scans before and after irreversible CO chemisorption.

RESULTS AND DISCUSSION

Figure 1 shows the influence of contact time on the percentage yield for the *n*-C_4 reaction in the pulse mode in the presence of hydrogen over the $W_{12}Z$ catalyst. The formation of methane is an indication that terminal C-C bond rupture, characteristic of acid cracking, is taking place on this catalyst. In Fig. 2, it can be seen that addition of 0.3 wt% Pt produces a catalyst about half order of magnitude more active than the Pt-free sample, but its selectivity toward isomerization is only doubled. With regard to C_2 production, internal C-C bond scission now dominates as expected in all-metal-catalyzed hydrogenolysis.

Figure 3 corresponds to the reaction of *n*-C_5 in the presence of hydrogen (pulse mode) over $W_{12}Z$. The main product is *iso*-C_5 and all other species follow the same trend as that observed in the *n*-C_4 reaction (Fig. 1). A comparison between the Pt-free catalyst runs (Figs. 1 and 3) reveals

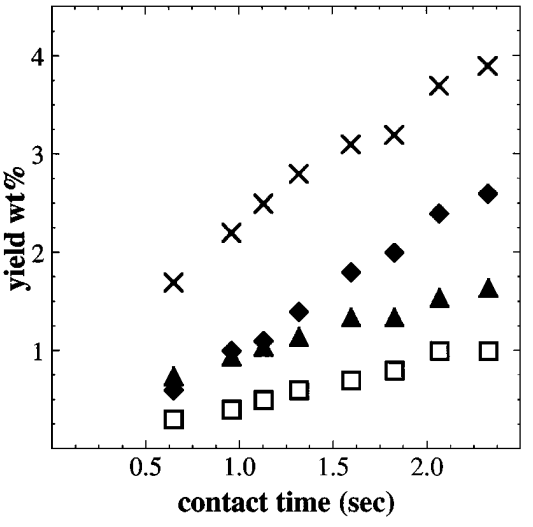

FIG. 1. Contact time vs conversion of *n*-C_4 on $W_{12}Z$: $T = 573$ K, $P_{H_2} = 580$ Torr, $P_{N_2} = 4420$ Torr; (✕) C_1, (❑) C_2, (▲) C_3, (◆) *i*-C_4.

that plots of isoparaffin production versus contact time essentially produce straight lines, whereas cracking products (including methane) show a tendency to level off that might be explained by the appearance of secondary reactions that eventually yield carbon-containing surface residues. Note that one should expect secondary gaseous products to increase more than linearly with contact time, but such "secondary products" may well be small amounts of coke, as we will discuss later.

Under the same conditions, the addition of Pt increases the overall activity, as well as the selectivity, toward isomerization for the reaction of *n*-C_5 over these catalysts much more markedly than for *n*-C_4, as shown in Fig. 4. Total conversion is greatly improved and the isomerization yield

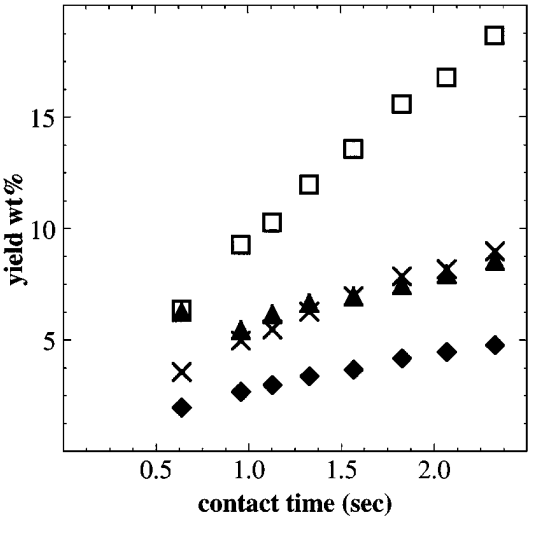

FIG. 2. Contact time vs conversion of *n*-C_4 on $Pt_{0.3}W_{12}Z$: $T = 573$ K, $P_{H_2} = 580$ Torr, $P_{N_2} = 4420$ Torr; (✕) C_1, (❑) C_2, (▲) C_3, (◆) *i*-C_4.

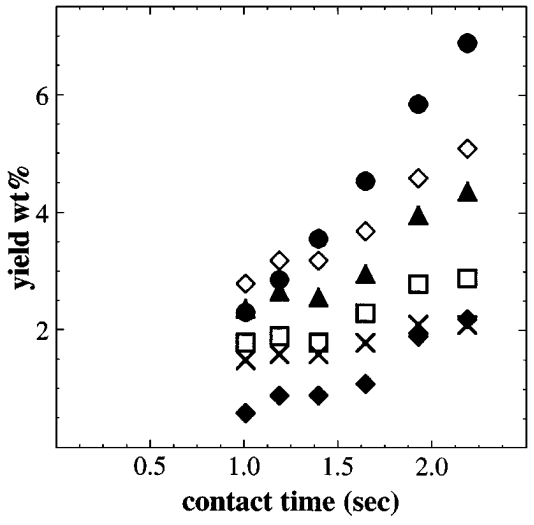

FIG. 3. Contact time vs conversion of n-C_5 on $W_{12}Z$: $T = 543$ K, $P_{H_2} = 580$ Torr, $P_{N_2} = 4420$ Torr; (✕) C_1, (❑) $C_2 \times 5$, (▲) $C_3 \times 5$, (◆) i-$C_4 \times 5$, (◇) n-$C_4 \times 5$, (●) i-C_5.

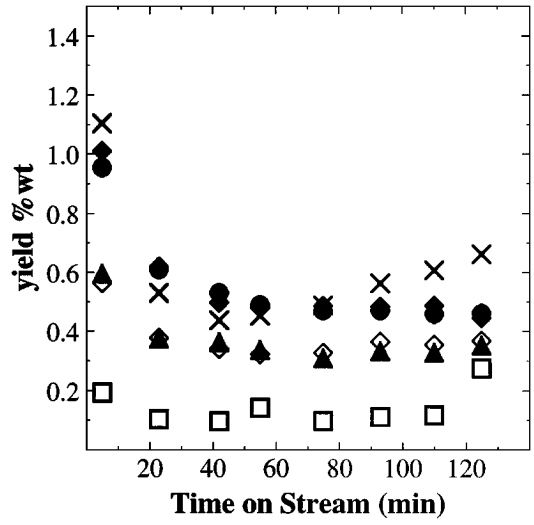

FIG. 5. Continuous n-C_5 flow reaction over $W_{12}Z$: $T = 543$ K, catalyst load = 700 mg, $P_{n\text{-}C_5} = 100.5$ Torr, $P_{H_2} = 374$ Torr, $P_{total} = 760$ Torr, feed rate per mass of catalyst = 0.4684 kg n-C_5 (kg cat)$^{-1}$ h^{-1}; (✕) C_1, (❑) C_2, (▲) C_3, (◆) i-C_4, (◇) n-C_4, (●) i-$C_5 \times 0.1$.

increases roughly one order of magnitude. Figures 5 and 6 correspond to the flow-mode experiments with n-C_5 in the presence of hydrogen at atmospheric pressure. For the Pt-free catalyst (Fig. 5) *iso*-products follow a trend that differs from that of C_1 and C_2. For the Pt-containing catalysts, the selectivity toward *iso*-C_5 is greatly increased (see Fig. 6). An important observation in that disproportionation products were not present in any experiment for the n-C_5 reaction; i.e., C_6 species were not detected. Interestingly, we have observed pentanes in our previous n-C_4 reaction studies under similar continuous flow experimental conditions (8,10). This suggests that n-pentane may undergo unimolecular rearrangement instead, as discussed below.

From the deactivation profiles depicted in Fig. 7 and assuming a deactivation rate of the form yield% $= \alpha t^n$, the deactivation exponent n for $Pt_{0.3}W_{12}Z$ is about three times higher than that of the $W_{12}Z$ catalyst. Thus, addition of Pt enhances the activity but does not appear to slow down deactivation at low pressures. We note, however, that the initial conversions were not the same, so that one should proceed with caution when comparing the deactivation profiles of the two catalysts.

The chemisorption experiments showed negligible CO and hydrogen uptakes for the samples used in these

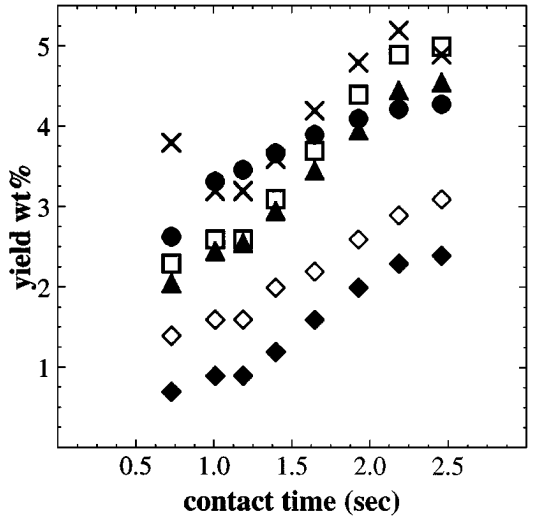

FIG. 4. Contact time vs conversion of n-C_5 on $Pt_{0.3}W_{12}Z$: $T = 543$ K, $P_{H_2} = 580$ Torr, $P_{N_2} = 4420$ Torr; (✕) C_1, (❑) C_2, (▲) C_3, (◆) i-C_4, (◇) n-C_4, (●) i-$C_5 \times 0.1$.

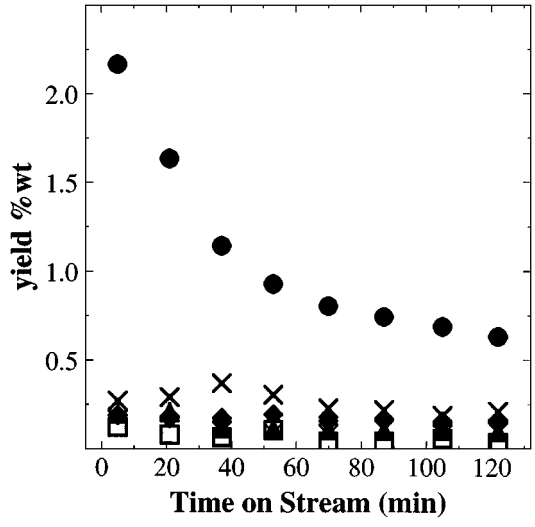

FIG. 6. Continuous n-C_5 flow reaction over $Pt_{0.3}W_{12}Z$: $T = 543$ K, catalyst load = 700 mg, $P_{n\text{-}C_5} = 100.5$ Torr, $P_{H_2} = 374$ Torr, $P_{total} = 760$ Torr, feed rate per mass of catalyst = 0.6245 kg n-C_5 (kg cat)$^{-1}$ h^{-1}; (✕) C_1, (❑) C_2, (▲) C_3, (◆) i-C_4, (◇) n-C_4, (●) i-$C_5 \times 0.1$.

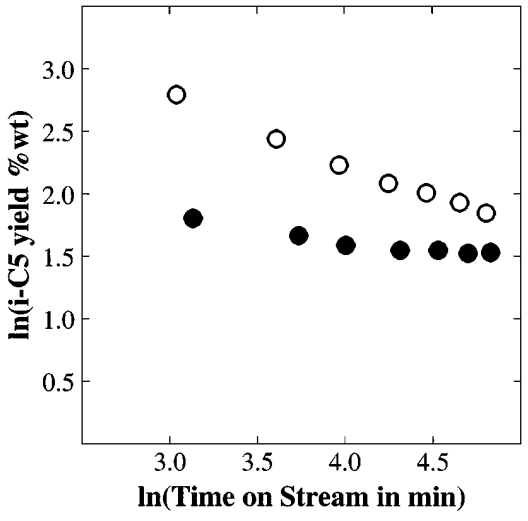

FIG. 7. Deactivation profiles: (○) $Pt_{0.3}W_{12}Z$, (●) $W_{12}Z$.

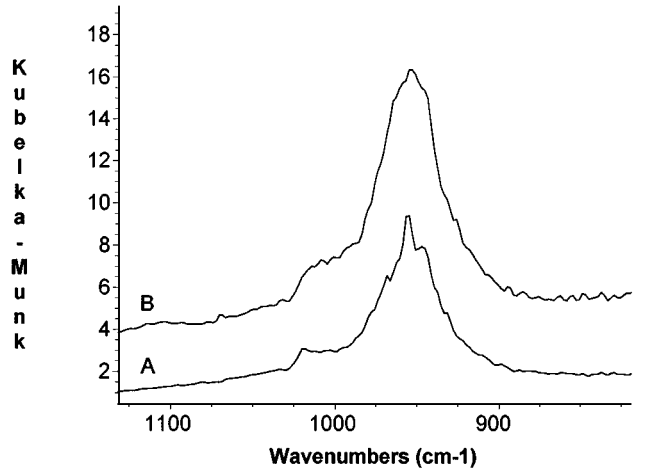

FIG. 9. $W_{12}Z$ DRIFTS spectra corresponding to W=O region at 623 K under nitrogen flow (A) prior to reduction and (B) after hydrogen reduction.

reaction studies. Therefore, to investigate the DRIFTS spectra of adsorbed CO, it was decided to use a sample from our previous work (8) with a Pt/W ratio eight times higher than the one used for the present reaction studies. This sample was labeled as $Pt_{1.2}W_6Z$. The results are shown in Fig. 8. The low dispersions resulting from calcination at 1096 K affected the signal/noise ratio. Nevertheless, the band centered at 2070 cm^{-1} has been assigned to linear CO adsorbed on Pt sites for platinum–zirconia (PtZ) catalysts and the band around 1855 cm^{-1} to the bridged CO (20). The intensity of the 2070 cm^{-1} for the tungstated catalyst is lower than that for the tungsten-free material. In addition, the absence of the typical bridged CO IR band in PtWZ could be explained by decoration of the Pt surface by partially reduced WO_x species. We have observed large Pt particles by means of transmission electron microscopy (ca 10–25 nm), but one should keep in mind that such particles, if surface-clean, should still present the expected linear (dominant) and bridged IR pattern typically observed in Pt catalysts, such as that of the tungsten-free material. The negligible CO and hydrogen adsorption of PtWZ, the very low linearly adsorbed CO DRIFTS signal, and the pronounced *n*-pentane deactivation profile under continuous flow point to the fact that, at least at low pressures, the Pt function is unlikely to display the conventional protective effect toward coking by hydrogen spillover. Rather, it appears that the key role of Pt is to produce a larger number of isomerization sites on WZ. The suppressed chemisorption characteristics of PtWZ prevented us from reporting reaction data in realistic turnover frequency units.

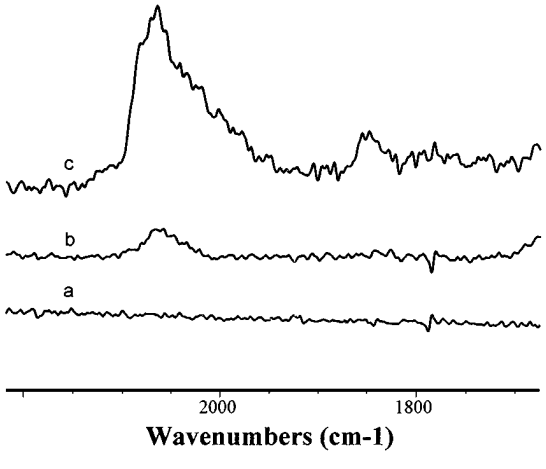

FIG. 8. DRIFTS spectra of CO adsorption on (a) $W_{12}Z$, (b) $Pt_{1.2}W_6Z$, and (c) $Pt_{1.2}Z$.

By comparing the DRIFTS spectra of our catalysts (Fig. 9) to those reported in the literature for bulk tungsten oxide species, bands around 960 and 1017 cm^{-1} may be assigned to terminal W=O (12). Very recently, Boyse and Ko (21) suggested that the presence of the 1020 cm^{-1} correlates with catalyst activity in WZ. Our *in situ* results reveal that this band becomes broader in the presence of hydrogen and shifts to lower frequencies. Since such red shifts were observed in the W=O stretching frequencies in partially reduced WO_x thin films (22), we conclude that partially reduced tungsten exists under reaction conditions. An important observation is that Pt is expected to facilitate the formation of such WO_x moieties.

Deactivation was not fully prevented for *n*-C_5, even in the pulse mode. Table 1 shows a small decrease in activity (more pronounced in terminal C-C bond rupture products) before and after the pulse sequence. Although curves in Fig. 3 and Fig. 4 are subjected to such modest deactivation, there is an interesting observation to be made. First, the same deactivation toward cracking (terminal C-C bond rupture) was observed in both $W_{12}Z$ and $Pt_{0.3}W_{12}Z$, indicating that this phenomenon is not due to the presence of Pt,

TABLE 1

Comparison of the Pulse Reactor Performance for n-C_5 on $Pt_{0.3}W_{12}Z$ before and after the Pulse Train in Fig. 4

	Product wt%					
	CH_4	C_2H_6	C_3H_8	i-C_4H_{10}	n-C_4H_{10}	i-C_5H_{12}
First pulse	3.767	2.325	2.207	0.687	1.407	26.332
Last pulse	2.338	1.903	1.885	0.556	1.216	27.465

Note. $T = 543$ K, $P_{H_2} = 580$ Torr, $P_{N_2} = 4420$ Torr. Contact time: 0.73 s.

but to conventional metallic hydrogenolysis. Furthermore, such behavior was not observed in the isomerization pathway, which suggests that the latter does not occur over the same type of catalytic sites as the cracking network. Note that in Figs. 1–4, isomerization responded nearly in a linear fashion with increasing contact time, the exception being perhaps Fig. 4, because the large conversion levels make the reactor behave as integral, not differential. Note that this is the only case in which the *iso*-C_5 yield decreases more rapidly than those of the lighter molecules, whereas the latter show sigma-shaped curves characteristic of species that are also formed by secondary reactions. This implies that *iso*-C_5 decomposes at high conversions to smaller hydrocarbons. For the pulse experiments, we have elected to compare the catalytic behavior of our samples under the same pressure, temperature, and contact time for a given reaction, rather than to attempt reaching the same conversion levels by varying the contact time. This is because we wanted to determine the effect of Pt addition on catalysts while minimizing deactivation effects. Figure 1, for example, shows that isobutane increases linearly with contact time, but the methane and propane production slows down with increasing contact time. As mentioned earlier, we take this as an indication that acid cracking and isomerization do not occur on the same active sites when the catalyst is relatively fresh (pulse studies). Similarly, Fig. 2 shows that both the ethane (a predominantly metal-catalyzed pathway) and the isobutane production from n-C_4 over the Pt-containing catalyst is somewhat more stable than terminal cracking.

We have reported in the past that small amounts of pentanes are produced during the isomerization of n-C_4 over PtWZ (10) under hydrogen at atmospheric pressure. Such products are commonly observed when a bimolecular intermediate is responsible for both isomerization and disproportionation. For acid-catalyzed isomerizations, n-C_5 represents the first linear paraffin that can undergo unimolecular skeletal rearrangement without having to generate a primary carbenium-like intermediate (9). A dimeric intermediate can either undergo isomerization or disproportionation by β-scission (10,11). We have previously shown that both Brønsted and Lewis acid sites are present upon hydrogen reduction of the catalyst (23,24). However, acidity alone may not account for the catalytic behavior of PtWZ. The spent catalysts preserve a deep blue coloration even after air exposure. This is commonly observed in electrochromic tungsten oxide films in tungsten intermediate oxides, and in some tungsten bronzes, which contain stable, delocalized W^{+5} centers (25). A small but detectable amount of tungsten reduction has been confirmed by X-ray absorption near edge spectroscopy at the W L_{III} edge (24). In fact, tungsten bronze chemistry has been suggested as an important component of the catalytic action of PtWZ (26). Partial tungsten reduction was also proposed as key for the n-C_5 isomerization activity of WZ (13). Given that Pt generally catalyzes the reduction of nonnoble metals by hydrogen spillover, the generation of a larger proportion of partially reduced centers may account for the higher n-C_5 isomerization activity of PtWZ with respect to the Pt-free material (see Figs. 3 and 4). Production of the so-called hydrogen bronzes by hydrogen spillover at room temperature by mechanical mixtures of platinum supported on alumina and WO_3 is a process known since the mid 1960s (27). By then, it was established that water played a key role in the hydrogen surface mobility (28). On the other hand, reduction of (noble-metal-free) WO_3 by molecular hydrogen at temperatures above 473 K has been reported by Weiss in 1935 (29).

Water molecules, produced during the reduction steps, in addition to form Brønsted acid sites (13) are likely to be responsible for hydrogen mobility in these catalysts. It has been reported that hydrocracking of *n*-heptane over tungsten oxide shows different reaction products, depending on the oxidation state of tungsten (30). Partial reduction of tungsten seems to play a role in the isomerization activity of tungstated zirconia, but highly active cracking sites are present when the surface of the catalyst is essentially free of coke.

Further analysis can be carried out by inspection of the activation energies measured in the pulse mode. These were measured by decreasing the temperature (thus minimizing the possibility of further deactivation) of the samples after the experiments shown in Figs. 1–4. Besides the result for C_3 production from *n*-butane over WZ that must be due to an artifact (e.g., C_3 FID signal near the detection limit) and for isopentane over PtWZ which reached 18% at the highest temperature employed, hydrogenolysis and cracking products show the general trend of higher activation energies than isomerization, as is normally expected. In Table 2, it

TABLE 2

Activation Energies

		Activation energy (kJ/mol)					
Feed gas	Sample	CH_4	C_2H_6	C_3H_8	i-C_4H_{10}	n-C_4H_{10}	i-C_5H_{12}
n-C_4	$W_{12}Z$	169	119	66	101	—	-
	$Pt_{0.3}W_{12}Z$	162	167	191	125	-	-
n-C_5	$W_{12}Z$	172	171	130	-	138	68
	$Pt_{0.3}W_{12}Z$	132	148	160	-	140	84

is also seen that the isomerization activation energies computed for *n*-C_5 are lower than those for *n*-C_4 isomerization beyond experimental error. This observation, coupled with the absence of disproportionation products from *n*-C_5 suggest that a transition in the reaction mechanism occurs when going from *n*-C_4 to *n*-C_5. The E_a values measured by the pulse technique compare well with our previously reported data (31). For example, the 101 kJ/mol *n*-butane isomerization value is close to 96 kJ/mol, as previously measured over PtWZ under flow conditions (31). Another reference point is the values reported by Leclercq *et al.* (32) on *n*-butane C-C bond rupture in the flow mode over Pt/Al_2O_3, which fell in the 125–160 kJ/mol range.

By comparing Figs. 3 and 4, the presence of Pt (a well-known catalyst for reduction of nonnoble metal oxides) favors the production of isopentane over that of degradation species. The presence of W makes Pt lose its ability to coordinate CO in a bridged fashion, which is consistent with both partial reduction to form WO_x and the presence of a Pt–WO_x interaction. We have previously shown that a reduction peak around 550 K appeared in the temperature-programmed reduction pattern of PtWZ, and that such a signal was not present in PtZ (24).

Platinum addition results in more active and more selective isomerization catalysts in the temperature range studied. Clearly, the number of active sites is affected, and one could tentatively propose that partially reduced tungsten centers are primarily responsible for isomerization, but such sites should apparently have less tendency to catalyze the degradation of the linear paraffin into smaller molecules than the strong acid sites present with or without Pt addition. Such tungsten centers are expected to be hydrated species acting as hydrogen reservoirs involved in the hydride transfer steps. Both Brønsted and Lewis acid sites are present after hydrogen reduction of WZ and PtWZ catalysts, as shown by previous pyridine DRIFTS studies (23, 24). However, this study shows that highly active cracking sites deactivate faster than the sites responsible for alkane isomerization.

CONCLUSION

A comparison between the *n*-butane and *n*-pentane reactions in the presence of hydrogen over Pt-free and Pt-loaded tungstated zirconia catalysts was made under identical conditions. The main role of the Pt function, which has very limited hydrogen and CO chemisorption capacities, is to create more isomerization sites, rather than to prevent catalyst deactivation. The PtWZ sample gave a hardly detectable CO DRIFTS signal, relative to its tungsten-free counterpart. This is in agreement with the idea that the Pt surface is likely to interact with the reducible oxide phase (WO_x). The latter behaves like tungsten-colored centers, as monitored by the behavior of W-O IR bands in the 1020–960 cm^{-1} range.

The strongest acid sites present on the clean surface of tungstated zirconia catalyze acid-cracking reactions preferentially, but, given their rapid deactivation, these are likely to play little or no role in the steady state performance of these catalytic materials. They are, however, expected to be responsible for coke deposition during the initial operation.

ACKNOWLEDGMENTS

Support by the donors of the Petroleum Research Fund (Grant 31067-AC5) is gratefully acknowledged. One of us (LMP) thanks the University of San Juan (Argentina) for financial support.

REFERENCES

1. Corma, A., and Martínez, A., *Catal. Rev. Sci. Eng.* **35**, 483 (1993).
2. Larsen, G., Lotero, E., Parra, R. D., Petkovic, L. M., Silva, H. S., and Raghavan, S., *Appl. Catal. A: Gral.* **130**, 213 (1995).
3. Corma, A., *Chem. Rev.* **95**, 559 (1995).
4. Hino, M., and Arata, K., *Chem. Lett.*, 971 (1989).
5. Hino, M., and Arata, K., *J. Chem. Soc. Chem. Commun.*, 1259 (1987).
6. Soled, S. L., *in* "AIChE 1994 Annual Meeting, San Francisco, Nov. 1994."
7. Soled, S. L., Gates, W. E., and Iglesia, E., U.S. Patent 5,422,327 (1995).
8. Larsen, G., Lotero, E., Raghavan, S., Parra, R. D., and Querini, C. A., *Appl. Catal. A: Gral.* **139**, 20 (1996).
9. Brower, D. M., *in* "Chemistry and Chemical Engineering of Catalytic Processes" (R. Prins and G. C. A. Schuit, Eds.). Sijthoff & Noordhoff, The Netherlands, 1980.
10. Larsen, G., and Petkovic, L. M., *J. Mol. Catal. A: Chem.* **113**, 517 (1996).
11. Rezgui, S., and Gates, B. C., *Catal. Lett.* **37**, 5 (1996).
12. Daniel, M. F., Desbat, B., and Lassegues, J. C., *J. Solid State Chem.* **67**, 235 (1987).
13. Santiesteban, J. G., Vartuli, J. C., and Chang, C. D., *J. Catal.* **168**, 431 (1997).
14. Blanchard, G., and Charcosset, H., *J. Catal.* **66**, 465 (1980).
15. Rouco, A. J., and Haller, G. L., *J. Catal.* **72**, 246 (1981).
16. Alvarez, W. E., and Resasco, D. E., *J. Catal.* **164**, 467 (1996).
17. Doraiswamy, L. K., and Sharma, M. M., "Heterogeneous Reactions: Analysis, Examples, and Reactor Design," Vol. 1. Wiley, New York, 1984.
18. Satterfield, C. N., "Mass Transfer in Heterogeneous Catalysis," MIT Press, Cambridge, MA, 1970.
19. Mears, D. E., *Ind. Eng. Chem. Process Des. Devel.* **10**(4), 541 (1971).
20. Ivanov, A. V., Kustov, L. M., Vasina, T. V., Kazanskii, V. B., and Zeuthen, P., *Kinet. Catal.* **38**(3), 403 (1997).
21. Boyse, R. A., and Ko, E. I., *J. Catal.* **171**, 191 (1997).
22. Paul, J-L., and Lassegues, J. C., *J. Solid. State Chem.* **106**, 357 (1993).
23. Larsen, G., Raghavan, S., Márquez, M., and Lotero, E., *Catal. Lett.* **37**, 57 (1996).
24. Larsen, G., Lotero, E., and Parra, R. D., *in* "11th Int. Congress on Catal. 40th Anniversary" Stud. Surf. Sci. Catal., Vol. 101 (J. W. Hightower and W. N. Delgass, Eds.), p. 543. Elsevier Sci., Amsterdam, 1996.
25. Wells, A. F., "Structural Inorganic Chemistry," 4th ed., Clarendon Press, Oxford, 1975.
26. Iglesia, E., private communication.
27. Khoobiar, S., *J. Phys. Chem.* **68**(2), 411 (1964).
28. Benson, J. E., Kohn, H. W., and Boudart, M., *J. Catal.* **5**, 307 (1966).
29. Weiss, J., *Trans. Faraday Soc.* **53**, 656 (1957). [And references cited therein]
30. Ogata, E., Kamiya, Y., and Ohta, N., *J. Catal.* **29**, 296 (1973).
31. Larsen, G., and Petkovic, L. M., *Appl. Catal. A: Gral.* **148**, 155 (1996).
32. Leclercq, G., Leclercq, L., and Maurel, R., *J. Catal.* **44**, 68 (1976).